Energy Reports 8 (2022) 6301–6320

Contents lists available at ScienceDirect

Energy Reports

journal homepage: www.elsevier.com/locate/egyr

Research paper

Sensitivity of energy performance to the selection of PCM melting temperature for the building located in Cfb climate zone

Abylaikhan Bozzhigitov, Shazim Ali Memon *, Indira Adilkhanova

Department of Civil and Environmental Engineering, School of Engineering and Digital Sciences, Nazarbayev University, Nur-Sultan 010000, Kazakhstan

ARTICLE INFO

Article history:
Received 18 January 2022
Received in revised form 3 April 2022
Accepted 25 April 2022
Available online xxxx

Keywords:
Phase change materials (PCM)
Cfb climate zone
Fanger predictive mean vote index
Energy consumption reduction (ECR)
Average savings drop (ASD)

ABSTRACT

In the present study, optimization of PCM layer thickness and melting temperature to increase the energy-saving potential of the office building located in eight cities in the Cfb climate zone was conducted using the Fanger model. The sensitivity of the energy savings to the selection of PCM melting temperature was quantitatively analyzed using a novel indicator of average savings drop. Additionally, the investigation of the effect of real PCMs on the energy performance of the building located in Cfb climate as well as the economic and environmental analyses were accomplished. The results showed that the PCM layer with a thickness of 2 cm reached the highest values of energy savings per unit thickness. The optimization of the PCM melting temperature revealed that PCM 22–25 were optimum for the whole Cfb climate zone and resulted in energy consumption reduction values of up to 37.6%. The sensitivity analysis showed that the steadiness of the outdoor climate conditions affects the sensitivity of the energy savings to the selection of PCM melting temperature. The analysis of real PCMs revealed that PCM 25-r demonstrated more efficient performance in all cities. Overall, it was concluded that the integration of PCM can be considered an economically and environmentally feasible solution.

1. Introduction

Building and construction industries are responsible for about one-third of the global energy consumed and around 40% of direct and indirect carbon dioxide emissions (IEA, 2019). A major part of the energy consumed by buildings is spent on heating and cooling needs. It is forecasted, that global energy consumption will keep on rising due to growing population and climate change (Souayfane et al., 2016). Therefore, enhancing the energy efficiency of the buildings and improving indoor thermal comfort conditions is one of the main objectives of global energy policy. In recent years, integration of latent heat thermal energy storage materials (LHTES) such as phase change materials (PCM) into the building envelope has become an innovative solution for reducing indoor temperature fluctuations, regulating energy consumption and as a consequence increasing the energy-saving potential of the building (Arıcıet al., 2020). PCMs represent materials possessing high heat capacity and have the property to absorb and release a large amount of energy during the phase transition process from a solid-state to a liquid state and vice versa (Peng et al., 2019).

Several studies about thermal and energy performance of PCM integrated buildings showed that the effectiveness of the PCM considerably depends on such factors as the amount of PCM, PCM melting temperature, and climate conditions. For example, Arıcıet al. (2020) numerically investigated the thermal performance of the PCM integrated building and tried to find an optimum location, PCM melting temperature, and PCM layer thickness for enhancing the building's energy performance for different climates of Turkey. The results showed that the annual optimum temperatures for Diyarbakır, Konya, and Erzurum were 20 °C , 25 °C and 16 °C respectively. For all cities, a PCM layer thickness of 20 mm was found to be optimum. Mohseni and Tang (2021) experimentally and numerically investigated the effectiveness of the PCM in improving thermal comfort conditions and optimizing the thickness and melting temperature of PCM for a building located in the city of Newcastle, Australia. The author considered PCMs with the melting temperature varying in the range from 19 °C to 29 °C , and PCM layer thicknesses of 5 cm and 10 cm. The results showed that PCM with a melting temperature of 21 °C and layer thickness of 10 cm placed on roof and external walls resulted in the best performance in terms of reducing the energy consumption. Tunçbilek et al. (2020) conducted an optimization study for PCM integrated office building for the climate

Abbreviations: ASD, Average Savings Drop; ADT, Adaptive Thermal Comfort Theory; EC, Energy Consumption; ECR, Energy Consumption Reduction; ES, Energy savings; HVAC, Heat Ventilation and Air Conditioning; LHTES, Latent Heat Thermal Energy Storage materials; PCM, Phase Change Materials; PMV, Predictive Mean Vote; PTHP, Packaged Terminal Heat Pump; SPP, Static Payback Period

* Corresponding author.
E-mail address: shazim.memon@nu.edu.kz (S.A. Memon).

https://doi.org/10.1016/j.egyr.2022.04.059

of the Marmara region (Turkey) classified as the Csa climate zone. The authors tried to determine the optimum location, thickness and melting temperature of the PCM for maximizing energy savings. According to the data obtained, the authors revealed that PCM melting temperature of 25 °C, which was equal to the upper setpoint temperature was optimum for the studied region. Additionally, the results showed that the PCM layer with a thickness of 23 cm placed closer to the inner surface of the wall was the best and helped to achieve energy savings of up to 12.8%. Kishore et al. (2020) numerically investigated the impact of PCM on the energy performance of the building, analyzed key conditions for effective application of the PCM, and tried to optimize PCM melting temperature and location for different climates of the US. The results showed that in Phoenix, Las Vegas, Baltimore, and Denver optimum PCM melting temperatures were 22 °C , 22 °C , 24 °C , and 24 °C respectively. For all cities, the PCM layer placed in the middle of the wall composition was found to be optimum. Markarian and Fazelpour (2019a) conducted multi-objective optimization to determine the optimum PCM type and location for enhancing the energy efficiency of the building located in different climates of Iran. The results of the study demonstrated that PCM 25 was the best in reducing cooling energy consumption, whereas PCM 21 was the optimum in decreasing heating energy demand. Jangeldinov et al. (2020) investigated the impact of PCM melting temperature on heating and cooling loads in different cities of warm-summer humid continental climates (Dfb). The results showed that in Kyiv and Stockholm PCM 21 resulted in the highest energy savings, while in Saint Petersburg, Moscow, Toronto, and Montreal PCM 24-PCM 26 demonstrated more effective performance. Lei et al. (2016) analyzed the effectiveness of the PCM in decreasing cooling energy consumption for the climate of Singapore using numerical simulations. The data showed that PCM 28 applied to the exterior surface of the wall was optimum. The authors highlighted that selection of the PCM melting temperature is crucial and it depends on the location of the PCM layer. Alam et al. (2017) compared the effect of passive and free cooling application methods of PCM for the residential building located in the climate of Melbourne (Australia) representing the Cfb climate zone utilizing Energy Plus software. The results of the study revealed that the free cooling approach was more effective, and PCM with a melting temperature of 25 °C resulted in higher values of peak temperature drop. The authors concluded that PCM melting temperature should be chosen based on the PCM application method. Additionally, they highlighted that for passive application of the PCM, optimum PCM melting temperature equals the average indoor air temperature, whereas for the free cooling application method it is equivalent to the average outdoor air temperature of the climate zone. Saffari et al. (2017a) conducted a simulation-based optimization of PCM melting temperature for improving the energy-saving potential of the building using Energy Plus and GenOpt software. The results showed that for Berlin, Paris, and Johannesburg optimum PCM melting temperatures were 24.38 °C, 24.06 °C, and 25.56 °C respectively.

From the literature mentioned above, it can be concluded that there are a lot of studies about the optimization of the amount of PCM and PCM melting temperature. However, there is a lack of studies evaluating the sensitivity of the energy savings to the PCM melting temperature and providing its quantitative analysis. Therefore, the present paper aims to address this research gap by optimizing the thickness and melting temperature of the PCM and providing a quantitative analysis of the sensitivity of energy savings to the PCM melting temperature for an office building located in eight cities of the Cfb climate zone using Design Builder software and setting Fanger model thermal comfort conditions. A novel indicator of average savings drop (ASD) was introduced for evaluating the conducted sensitivity analysis. The impact of outdoor climate conditions on the sensitivity of energy savings to the selection of PCM melting temperature was evaluated. Additionally, an investigation of the effect of real PCM melting temperature on the energy performance of the PCM integrated building located in the Cfb climate zone as well as economic and environmental analyses of PCM integrated buildings were conducted.

2. Methodology

2.1. Climate region

The temperate oceanic climate region (Cfb by Koppen classification) is characterized by warm summer, mild winter, and mostly rainy weather. The temperature in this region fluctuates between −3 °C and +18 °C throughout the year. The location of the Cfb climate zone on the world map is shown in yellow color in Fig. 1. Based on the population and economic importance, eight cities located in different countries were selected. Table 1 contains detailed information about selected cities.

2.2. Building model

For analysis, a flat-roof three-story office building with a base area of 1000 m^2 and a total height of 9.9 m (3.3 m per story) was used. Each side of the story contains five windows with the dimensions of 1. 5 m × 3 m each placed 0.9 m above the floor. Every window consists of two glass panels separated by an air gap of 6 mm. Each glass panel has a thermal conductivity of 0.9 W/m-K and a thickness of 6 mm. A door with a size of 2.4 m × 3 m is placed on the east wall. Fig. 2 shows the building selected for analysis. Exterior wall and roof compositions were extracted from the study of Saffari et al. (2016). External walls consist of four layers: plasterboard with a thickness of 12 mm, PCM layer with a thickness varying from 20–100 mm, and 200 mm, fiberglass with a thickness of 66 mm, and wood siding of 9 mm. The roof also consists of four layers: polyurethane layer of 6 mm, PCM layer varying from 20–100 mm, and 200 mm, insulation layer with the thickness of 20 mm, and gypsum board of 0.0127 mm. For both the external wall and roof, the PCM layer was placed right after the inner layer. The thermophysical properties of the materials used for both wall and roof compositions are shown in Table 2. The infiltration rate was set to 0.5 ACH.

2.3. PCM characteristics

Initially, for analysis, fictitious PCMs with the density of 860 kg/m^3, the specific heat of 1970 J/kg-K, the conductivity of 0.2 W/m-K and latent heat of 219 kJ/kg were used. The melting temperature of the selected PCM ranged from 18 °C to 30 °C with the 1 °C step. Each PCM has a phase change temperature range of 4 °C, so that for PCM 18 the melting temperature range varies from 16 °C to 20 °C, while for PCM 30 it was ranging from 28 °C to 32 °C . Fig. 3 represents the enthalpy temperature curves for selected fictitious PCMs.

2.4. Numerical simulations

The analysis was accomplished by means of Design Builder Software representing a comprehensive interface built over Energy Plus Software. To simulate materials with changing thermo-physical properties such as PCM, one-dimensional Conduction Finite Difference (ConFD) algorithm was selected. A fully implicit scheme was applied in combination with the enthalpy–temperature function defined by the user. The heat transfer

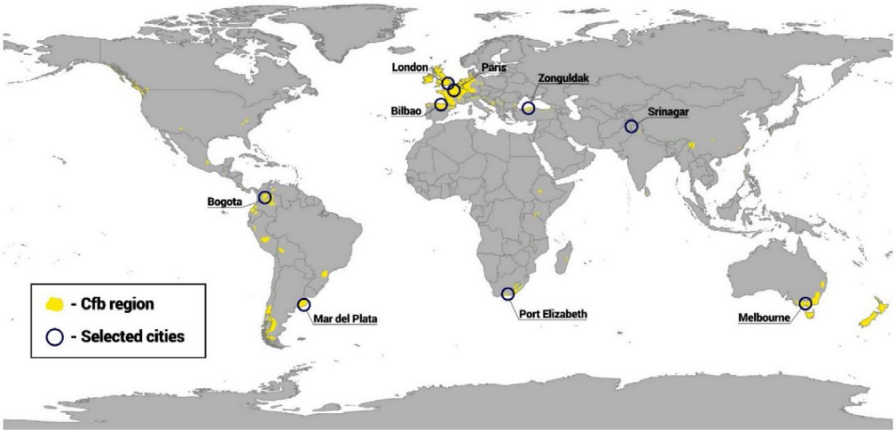

Fig. 1. Area of Cfb region and location of selected cities.

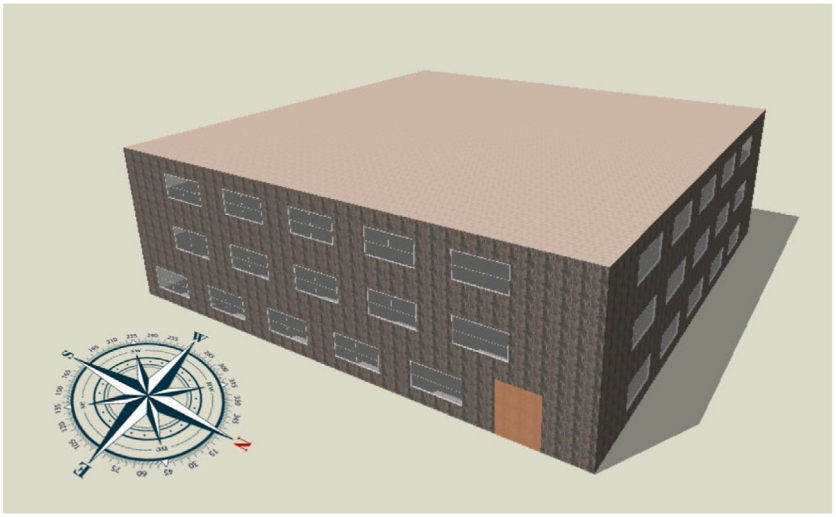

Fig. 2. Building model in Design Builder.

Table 1
List of selected Cfb cities.

City	Country	Status	Latitude	Longitude
Melbourne	Australia	Capital of state	−37.840935	144.946457
Paris	France	Capital city	48.864716	2.349014
Bogota	Colombia	Capital city	4.624335	−74.063644
Bilbao	Spain	The administrative center of the province	43.262985	−2.935013
Mar del Plata	Argentine	Port city	−37.979858	−57.589794
Zonguldak	Turkey	Capital of province	41.451733	31.791344
Srinagar	India	Capital of state	34.083656	74.797371
Port Elizabeth	RSA	Port city	33.991360	25.656912

Table 2
Characteristics of building materials used.

Material	Conductivity, W/m-K	Specific Heat, J/kg-K	Density, kg/m^3	Thickness, mm
Wall				
Plasterboard (Inner layer)	0.16	840	950	12
PCM	0.2	1970	860	20–100, 200
Fiberglass	0.04	840	12	66
Wood siding (Outer layer)	0.14	900	530	9
Roof				
Polyurethane (Inner layer)	0.0305	1381	1144	6
PCM	0.2	1970	860	20–100, 200
Insulation	0.034	883	12	20
Gypsum board (Outer layer)	0.16	1090	800	0.0127

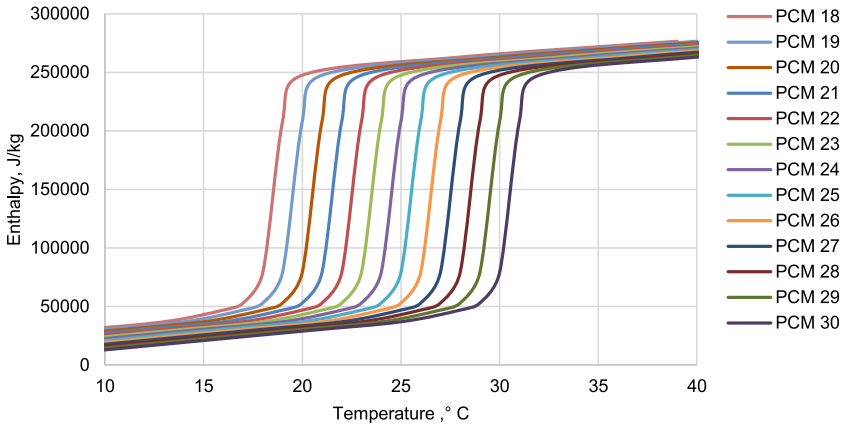

Fig. 3. Enthalpy–temperature curves for PCM 18–PCM 30.

equation used for a fully implicit scheme can be derived from the approximation of the one-dimensional diffusion equation (Anon, 2006):

$$\rho c \frac{dT}{dt} = \frac{d}{dx}\left(k \frac{dT}{dx}\right) \tag{1}$$

Where:
ρ — *density*
c — *specific heat*
T — *temperature*
t — *time*
x — *distance in direction of diffusion*

k — *thermal conductivity*

There are three methods of approximation of differential equation such as central, forward, and backward difference (Hyoung Kyu, 2015):

$$\frac{df(x)}{dx} \approx \frac{f\left(x+\frac{\Delta x}{2}\right) - f\left(x-\frac{\Delta x}{2}\right)}{\Delta x} \text{- first order central difference} \tag{2}$$

$$\frac{df(x)}{dx} \approx \frac{f(x+\Delta x) - f(x)}{\Delta x} \text{- first-order forward difference} \tag{3}$$

$$\frac{df(x)}{dx} \approx \frac{f(x) - f(x-\Delta x)}{\Delta x} \text{- first-order backward difference} \tag{4}$$

These approximations were applied to diffusion Eq. (1) to obtain the equation used in the Energy Plus software. First, the temperature variation with time in Eq. (1) was approximated by backward difference (4) on i-node and j-time step.

$$\left(\frac{dT}{dt}\right)_i^j \approx \frac{T_i^j - T_i^{j-1}}{\Delta t} \tag{5}$$

Then the central difference approximation (2) was applied to the second derivative of temperature with distance x:

$$\left(\frac{d}{dx}\left(k\frac{dT}{dx}\right)\right)_i^j \approx \frac{\left(k\frac{dT}{dx}\right)_{i+\frac{1}{2}}^j - \left(k\frac{dT}{dx}\right)_{i-\frac{1}{2}}^j}{\Delta x} \tag{6}$$

Using forward difference approximation (3) gave:

$$\left(k\frac{dT}{dx}\right)_{i+1/2}^j \approx k_+ \frac{T_{i+1}^j - T_i^j}{\Delta x} \tag{7}$$

$$\left(k\frac{dT}{dx}\right)_{i-1/2}^j \approx k_- \frac{T_i^j - T_{i-1}^j}{\Delta x} \tag{8}$$

Where:

k_+ *is thermal conductivity between i and* $i+1$
k_- *is thermal conductivity between i and* $i-1$.

Rearranging Eq. (6) with Eqs. (7) and (8) led to:

$$\left(\frac{d}{dx}\left(k\frac{dT}{dx}\right)\right)_i^j \approx \frac{\left(k\frac{dT}{dx}\right)_{i+1/2}^j - \left(k\frac{dT}{dx}\right)_{i-1/2}^j}{\Delta x} \approx \frac{k_+ \frac{T_{i+1}^j - T_i^j}{\Delta x} - k_- \frac{T_i^j - T_{i-1}^j}{\Delta x}}{\Delta x} \tag{9}$$

Finally applying Eqs. (5) and (9) to Eq. (1) gave the 1st order fully implicit equation algorithm used in Energy Plus (2022), which is:

$$C\rho\Delta x \frac{T_i^j - T_i^{j-1}}{\Delta t} = k_+ \frac{T_{i+1}^j - T_i^j}{\Delta x} + k_- \frac{T_{i-1}^j - T_i^j}{\Delta x} \tag{10}$$

The variation of thermal conductivity (k) with temperature (t) in the algorithm is given by:

$$k_t = k_{20} + K\,(t - 20) \tag{11}$$

Where:
k_{20} is the value of thermal conductivity at 20 °C
K is the change in conductivity per degree temperature difference from 20 °C (Energy Plus, 2022).

Specific heat capacity of PCM is changing at each time step in accordance with the following formula (Energy Plus, 2022):

$$C_p = \frac{h_i^j - h_i^{j-1}}{T_i^j - T_i^{j-1}} \tag{12}$$

where h (kJ/kg) is a specific enthalpy provided by a user as a function of temperature.

Tabares-Velasco et al. (2012) validated the reliability of Energy Plus in simulating PCM models and suggested some guidelines to improve its operation in the software. According to the authors, the time step should be less or equal to 3 min. Additionally, to produce more accurate hourly results, a smaller nodal space (less than 1/3 of the default value) should be used. For the present study, the time step of 2 min was selected.

2.5. Validation

In order to validate the reliability of the Design Builder model in simulating PCM, the experiment conducted by Cui et al. (2015) was modeled and simulated in the Design Builder software. In the experiment, Cui et al. (2015) used a lightweight aggregate concrete cubicle (Fig. 4) with the dimensions of 500 mm × 500 mm × 500 mm and a thickness of 20 mm for investigating the impact

Fig. 4. Experimental model (Bimaganbetova et al., 2019).

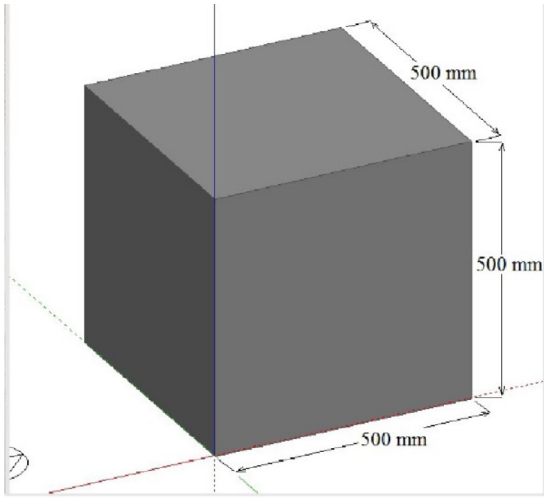

Fig. 5. Numerical model (Bimaganbetova et al., 2019).

of the PCM having the melting temperature of 23 °C on inside air temperature fluctuations in the climate of Shenzhen, China. Therefore, the model with the same dimensions was designed in the Design Builder software (Fig. 5) and the weather file of Shenzhen city was used. The analysis was accomplished for 48 h. Fig. 6 summarizes experimental and simulation-based results of inside air temperature. Based on the data presented, the discrepancy between experimental and simulation results was less than 4.5%. The deviation between numerical and experimental data can be a consequence of the simplification of the model and uncertainties linked to measurements. Some studies (Mi et al., 2016; Markarian and Fazelpour, 2019b; Alam et al., 2014) also found that the difference between experimental and numerical simulation results was up to 5%.

2.6. Thermal comfort model

Thermal comfort represents a condition of the mind expressing human satisfaction with the thermal environment. The are several approaches to measure thermal comfort conditions: operative temperature, adaptive thermal comfort theory (ADT), and Fanger's predictive mean vote (Saffari et al., 2016). Operative temperature represents a temperature sensed by people. It is calculated as a combination of mean radiant temperature and air temperature (Designing Buildings, 2020). The adaptive thermal comfort model is based on the idea that outdoor climate conditions influence indoor comfort conditions and occupants can adapt themselves to different temperatures in various periods of the year. The model is applicable to occupant controlled, naturally ventilated buildings. In ASHRAE-55 2010 (AHSRAE-55-2010, 2010) outdoor air temperature is used as the main factor for calculating the 80% and 90% thermal comfort satisfaction ranges. Fanger model was developed on the assumption that thermal comfort depends on the occupant's skin temperature and sweat secretion, and thermal comfort is reached only in the case when these two factors were balanced (Santamouris, 2014). Conducting climate chamber experiments, Fanger concluded that thermal comfort can be determined using metabolic rate, clothing insulation and occupant's environmental conditions (Djongyang et al., 2010). Using data obtained from the climate chamber experiment on 1296 Danish students, Fanger expanded the thermal comfort equation. The resulting equation was based on the four physical factors (such as air temperature, mean radiant temperature, air velocity and air humidity) and two personal factors (such as clothing insulation and metabolic rates of daily activities) related to the ASHRAE thermal seven-point sensation scale; it is known as the predictive mean vote (PMV) index. Thus, the Fanger PMV index represents an average vote of a large group of people on the ASHRAE thermal seven-point sensation scale (Table 3) (AHSRAE-55-2010, 2010). The Fanger model is one of the oldest and the most widely used thermal comfort models (Zhao et al., 2021). Therefore, in the present study, it was used as the thermal comfort model. Fig. 7 provides a schematic representation of the factors affecting the Fanger PMV index.

Table 3
Sensation categories by PMV (Energy Plus, 2022).

PMV value	Sensations
+3	Hot
+2	Warm
+1	Slightly warm
0	Neutral
−1	Slightly cool
−2	Cool
−3	Cold

2.6.1. HVAC

For analysis, Packaged Terminal Heat Pump (PTHP) HVAC system was used. PTHP system consists of DX heating and cooling coils, an air fan and an additional humidistat controller (Design Builder, 2020). The HVAC system operated 24 h per day, 7 days per week so that the comfort conditions were held permanently. The Fanger model can be applied when the detailed HVAC option is switched on. This option allows controlling indoor thermal comfort conditions using Fanger PMV heating and cooling setpoints instead of usual temperature setpoints. Following ASHRAE-55 2010 (AHSRAE-55-2010, 2010) standard, the PMV cooling and heating setpoints were set as +0.5 and −0.5 respectively. The clothing insulation values were set to 0.5 clo and 1.0 clo for the summer and winter periods respectively, while the metabolic rate was set to 127 W/person.

2.6.2. Inner surface analysis

In order to evaluate the effectiveness of the PCM in improving the thermal comfort conditions, an inner surface analysis was conducted. The gist behind this method is that the temperature of the PCM layer is assumed to be approximately equal to the inner surface temperature of the wall, because the PCM layer is located closer to the inner layer of the wall. The whole evaluation process can be described in two cases. In the first case, called "HVAC" the HVAC system is switched on, while no PCM layer is applied. In the

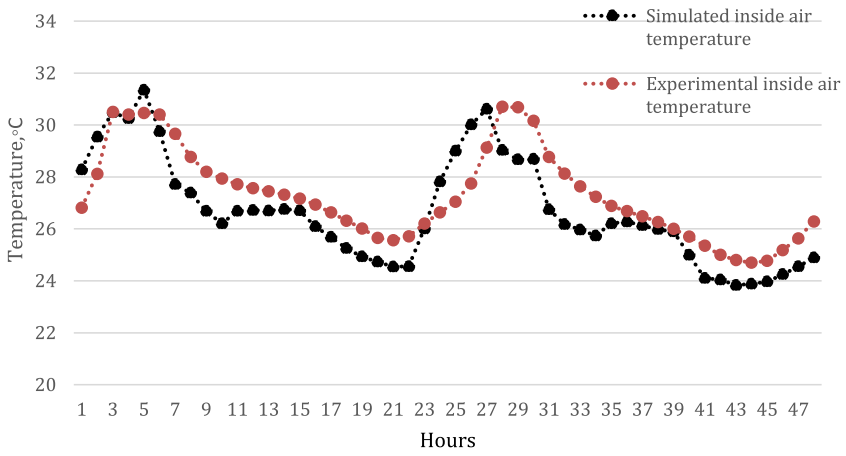

Fig. 6. Experimental vs simulation-based inside air temperature values (Kenzhekhanov et al., 2020).

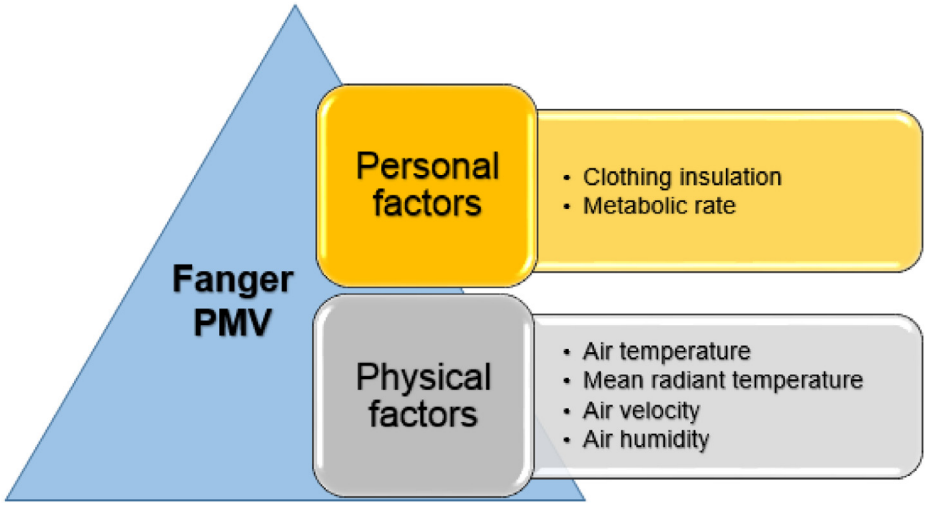

Fig. 7. Factors affecting Fanger PMV index.

second case called "PCM", the HVAC system was switched off, and the PCM layer was applied.

Analyzing the inner surface temperature of the PCM when the HVAC system is switched off allows assessing the real performance of PCM in improving the thermal comfort conditions while considering the inner surface temperature of the wall when no PCM is applied and the HVAC system is switched on allows evaluating the performance of the HVAC system.

In the periods when the temperature for the PCM case is close to the temperature for the HVAC case (left green rectangle in Fig. 8), it means that PCM demonstrates a performance similar to the HVAC system and it is effective in supporting thermal conditions that in turn results in the higher energy savings. In the periods when there is a considerable difference between HVAC and PCM temperature values (right red rectangle in Fig. 8), the PCM demonstrates less effective performance.

2.7. Effect of the amount of PCM on the energy performance

The effectiveness of PCM in improving the energy performance of the building strongly depends on such factors as the amount of PCM applied to the building envelope. In the present study, the optimization of the PCM layer thickness was accomplished. PCM layer thicknesses varied from 2 cm to 10 cm with the increment of 1 cm and one more case with a PCM layer thickness of 20 cm were considered. As performance indicators energy savings and energy savings per unit thickness were considered. Energy savings (ES) represent the amount of energy saved, once the PCM layer is applied to the building envelope. It is calculated as the difference between the energy consumption (EC) of the building without PCM and the energy consumption of the building integrated with PCM.

$$ES = EC(without\ PCM) - EC(with\ PCM) \tag{13}$$

To check the effectiveness of PCM layer thickness, the amount of energy savings per unit thickness was calculated. For this purpose, the ES obtained for each case was divided by thickness value.

2.8. Effect of PCM melting temperature on the energy performance

In addition to the amount of PCM, the effectiveness of the PCM in improving the energy performance of the building depends on the PCM melting temperature. In the present study, the optimum PCM melting temperature for each city was determined. For analysis, PCMs with the melting temperature range varying from 18 °C to 30 °C were considered. The optimization process was based on energy savings (ES) and energy consumption reduction (ECR). Annual energy consumption reduction (ECR) represents the percentage of the energy saved once the PCM layer is applied to the building envelope. It is calculated using the following

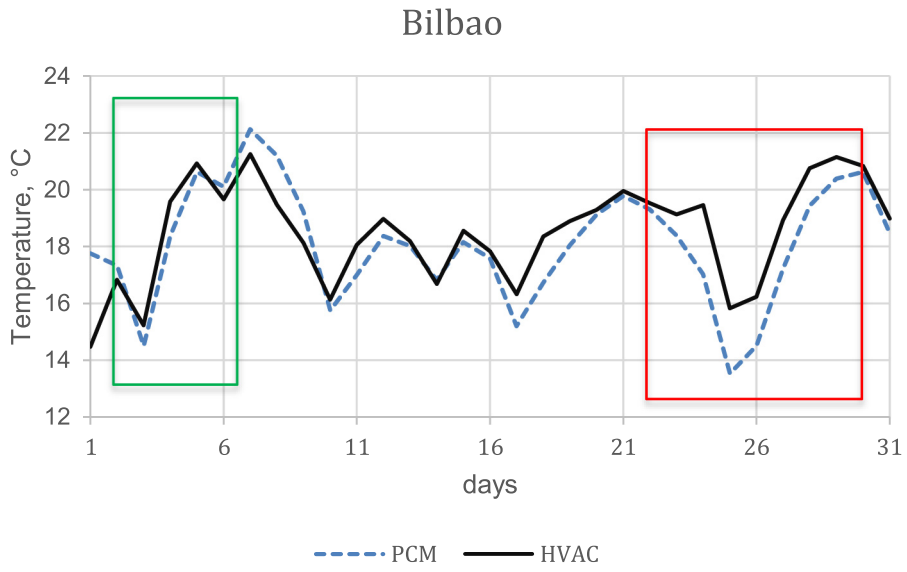

Fig. 8. Daily inner surface analysis example for December.

formula:

$$ECR = \frac{EC\ (without\ PCM) - EC(with\ PCM)}{EC(without\ PCM)} x100\% \quad (14)$$

2.9. Sensitivity analysis

In order to quantify the sensitivity of the energy performance of the building to the selection of the PCM melting temperature, a novel indicator of average savings drop (ASD) was introduced. Average savings drop (ASD) represents a change in annual energy consumption reduction per 1 °C change in the optimum PCM melting temperature. It is calculated as the ratio of the difference in energy consumption reduction (ECR) values of the most and least effective PCMs to the difference in melting temperature (T_{most} and T_{least}) of the most effective and least effective PCMs. Higher ASD values show higher sensitivity of the energy savings to the selection of the PCM melting temperature.

$$ASD = \left|\frac{ECR_{most} - ECR_{least}}{T_{most} - T_{least}}\right| \quad (15)$$

To evaluate the impact of outside climate conditions namely outside air temperature and direct solar radiation on the ASD values, the steadiness of the outside air temperature and direct solar radiation was determined through standard deviation. The formula of standard deviation is presented below:

$$x_{ave} = \frac{\sum_1^{365} x_i}{365} \quad (16)$$

$$St.Dev = \sqrt{\frac{1}{365} \times \sum_1^{365} (x_i - x_{ave})^2} \quad (17)$$

Where:
x_i — *daily samples (temperature or solar radiation)*
x_{ave} — *annual average of daily samples*
$St.Dev$ — *standard deviation of daily samples*

2.10. Real PCMs

Initially, the fictitious PCMs were used for comparative and optimization purposes due to the varying properties of the real PCMs. After completing a fictitious PCM analysis, it was decided to evaluate the impact of real PCMs on the energy performance of the building for the cities representing the Cfb climate zone. Inorganic materials such as salt hydrates are widely used due to their non-flammability, high latent heat, good thermal conductivity and comparatively low cost (Xu et al., 2017). However, salt hydrates experience supercooling over the process of releasing latent heat which limits their practical application (Xu et al., 2017). Due to outweighing benefits of the organic PCMs such as chemical stability, safety, corrosion resistance, good latent heat of fusion, and absence of tendency to supercooling or segregation (Mathew et al., 2019), four commercial organic PCMs with available enthalpy–temperature curves were selected. Based on the results of Section 3.3 real PCMs with the melting temperature of 21 °C, 22 °C, 24 °C, and 25 °C were considered. Since the manufacturer did not provide thermophysical properties and enthalpy–temperature curves for real PCM with the melting temperature of 23 °C, PCM with this melting temperature was not used for analysis. The main properties of the selected materials are summarized in Table 4. Fig. 9 represents the enthalpy–temperature curves provided by the manufacturer (Rubitherm, 2020).

2.11. Economic analysis and environmental impact of PCM

To investigate the economic feasibility of the PCM integrated building, the static payback period (SPP) was calculated using the following formula:

$$SPP = \frac{V \times \rho \times C_1 + A \times C_2}{ES \times C_3} \quad (18)$$

Where V is the volume of the used PCM in m^3, ρ is the density of the PCM in kg/m^3, C_1 is the cost of PCM in USD/m^3, A is the area of the PCM in m^2, C_2 is the cost of installation in USD/m^2, ES is the amount of energy saved in kWh, and C_3 is the cost of electricity in USD/kWh. The total area of PCM was determined by adding the roof area and area of all external walls (excluding windows) and was found to be equal to 1982.15 m^2. The volume of PCM was determined by multiplying the total area by the optimum PCM layer thickness. It was calculated after the optimum PCM layer thickness was selected in Section 3.1. The price of PCM and installation cost equal to 0.7 USD/kg and 5 USD/m^2 respectively were used for analysis; the values were adopted from the study of Saffari et al. (2016). The average electricity cost per kWh was individually found for each city. To calculate the amount of CO_2 reductions produced by energy consumption reductions, the values of CO_2 emissions per kWh were used from OECD (2019).

Table 4
Properties of real PCMs.

Name	Type	Melting temperature, °C	Heat storage capacity, kJ/kg	Density, kg/m^3	Heat conductivity, W/m K	Specific heat, kJ/kg K	Ref.
PCM 21-r	Organic	21	190	880	0.2	2000	Rubitherm (2020)
PCM 22-r	Organic	22	190	880	0.2	2000	Rubitherm (2020)
PCM 24-r	Organic	24	160	880	0.2	2000	Rubitherm (2020)
PCM 25-r	Organic	25	210	880	0.2	2000	Rubitherm (2020)

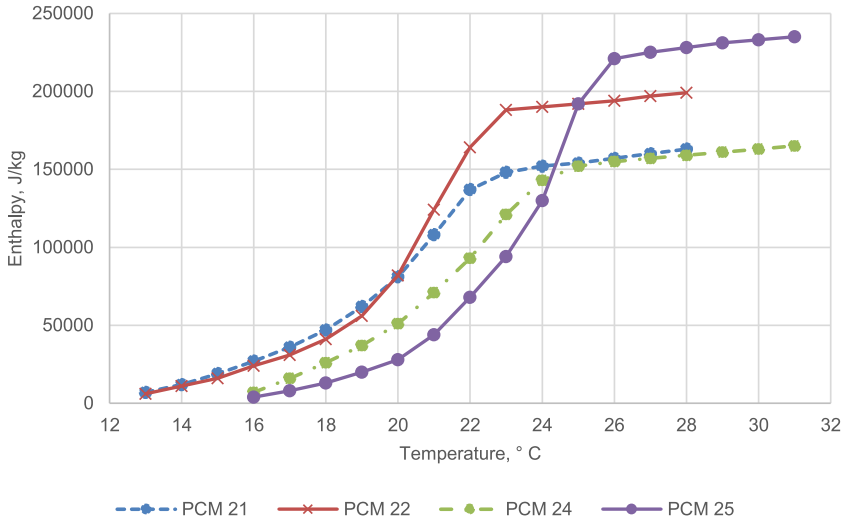

Fig. 9. The enthalpy–temperature curve for real PCM.

3. Results and discussion

3.1. PCM thickness optimization

In this section, the impact of PCM thickness on the annual energy consumption of the building was investigated for selected cities. Additionally, the optimum PCM layer thickness resulting in the highest energy savings was determined. For analysis, PCM with a melting temperature of 23 °C was used. Overall, 9 cases where PCM thickness varied from 2 cm to 10 cm with the increment of 1 cm and one more case with a PCM layer thickness of 20 cm were considered.

Ramakrishnan et al. (2016) tried to optimize the factors affecting PCM effectiveness in enhancing the thermal comfort conditions inside the building located in several Australian cities during the summer period. The results showed that increasing the thickness of the PCM notably improved thermal comfort conditions inside the building. However, it resulted in a decrease in thermal storage efficiency. Ascione et al. (2014) studied the impact of the PCM thickness on the energy consumption of the PCM integrated building located in five Mediterranean climates. Four different thicknesses of the PCM layer were considered: 0.5 cm, 1 cm, 2 cm, and 3 cm. It was revealed, that with the raising thickness, the cooling energy demand decreased. Thus, the PCM layer with a thickness of 3 cm resulted in the highest energy savings. However, Ascione et al. (2014) mentioned that further raising of the PCM layer thickness was not economically beneficial. The reason behind this was that the thicker PCM layer could not provide noticeable improvements in the comfort conditions, while the investment cost was increasing. Increasing the PCM layer thickness results in the rise of the PCM volume which in turn leads to higher prices spent on the PCM. However, the increase of the PCM layer does not produce higher energy savings, which in turn makes thicker PCM layers less cost-effective.

Therefore, to check the effectiveness of the thicker PCM layers, the amount of energy savings per unit thickness was calculated. It allowed a detailed evaluation of the impact of each PCM layer thickness increment on the energy savings. The results are presented in Fig. 10. Based on the data obtained, it is seen that for all cities the amount of energy savings per unit thickness got lower with the increase in the thickness of the PCM layer. For example, in Srinagar, the application of the PCM layer with the thickness of 2 cm resulted in energy savings of 10 142 kWh/cm, while for the thickness of 20 cm, it was 2061 kWh/cm. It implies that each newly added increment of the PCM layer had less impact on energy savings compared to the previous ones. Thus, the application of the thinner PCM layer is more efficient since it results in higher energy savings per unit thickness and as a result lower investment costs. Lei et al. (2016) came to a similar conclusion in their study about the effect of PCM on the energy performance of the PCM integrated building in Singapore. The authors scrutinized the influence of the amount of PCM on the heat gain reduction varying the thickness of the PCM layer from 3 mm to 20 mm for both exterior and interior locations. The data showed that with the incrementing thickness the heat gain reduction rate per mm of the thickness got lower.

Overall, based on the results obtained it was noticed that for the present study PCM layer of 2 cm is the optimum solution for all cities. It is worth mentioning that despite the relationship between ES per unit thickness and PCM layer thickness demonstrated declining trends for all cities selected for analysis, the absolute values of ES per unit thickness for specific PCM layer thickness varied from city to city The possible reason behind this is that the selected cities represent different climate conditions. Ahangari and Maerefat (2019) emphasized the strong dependence of PCM performance on the climate conditions of the studied area. Therefore, the optimization of PCM melting temperature for the selected cities was presented in Section 3.3.

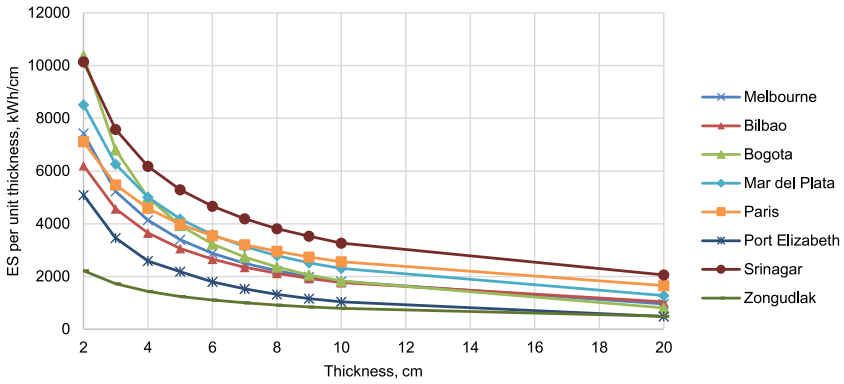

Fig. 10. Energy savings per unit thickness for PCM layer thicknesses of 2–10 cm, 20 cm.

3.2. Analysis of the impact of thin and thick PCM layers on energy performance

This section provides a more detailed analysis of the impact of thin and thick PCM layers on the energy performance of the building. For this purpose, the monthly energy consumption of the building integrated with PCM layers having a thickness of 2 cm and 20 cm were compared. Fig. 11 summarizes the results of the energy consumption for thin and thick PCM layer thickness cases for all cities. Based on the results obtained it is seen that in some months PCM layer with a thickness of 2 cm demonstrates a more effective performance resulting in less energy consumption.

To analyze the performance of 2 cm and 20 cm PCM layers, inner surface analysis was accomplished. For demonstration purposes, the cities of Melbourne and Mar del Plata were selected. For each city, one month when PCM layer with the thickness of 20 cm resulted in more effective performance and one month when PCM layer with the thickness of 2 cm demonstrated more effective performance were selected. For Melbourne, these months were January and May respectively, while for Mar del Plata such months were July and April respectively. Fig. 12 summarizes the results of the inner surface analysis for Melbourne and Mar del Plata for January and July respectively. According to the results presented, it can be noticed that the 20 cm PCM layer demonstrates performance similar to the HVAC case. It means that the application of the 20 cm PCM layer in these months supported the thermal comfort conditions within the thermal comfort range which in turn leads to energy savings. As for the 2 cm PCM layer, then it works against the HVAC system, which demonstrates a less effective performance in these months leading to higher values of energy consumption. Fig. 13 demonstrates the results of the inner surface analysis for Melbourne and Mar del Plata in May and April respectively. Based on the data presented it can be observed that in these months, the 2 cm PCM layer inner surface temperature is closer to the temperature for the HVAC case, while the 20 cm PCM layer works against HVAC. Overall, the results of the inner surface analysis clearly explain the reason behind more effective performance in terms of energy savings for 20 cm PCM and 2 cm PCM cases in various months.

3.3. PCM melting temperature optimization

In this section, the effect of the PCM melting temperature on the energy performance of the PCM integrated building located in different cities of the Cfb climate zone was investigated. The optimization of the PCM melting temperature was based on the annual energy savings. For analysis, PCMs with melting temperatures ranging from 18 °C to 30 °C were considered. Based on the results of the previous section, a PCM layer with a thickness of 2 cm was used.

The results of the energy savings and ECR for each PCM melting temperature for all cities are shown in Fig. 14. From the results presented it can be seen that all PCMs notably improve the energy performance of the building in all cities. Overall, PCMs with a melting temperature in the range from 22 °C to 25 °C resulted in slightly better performance, while PCMs with lower and higher melting temperatures were less efficient. For example, in Bilbao and Srinagar, PCM 22 resulted in the highest energy savings of 12 460 kWh and 20 468 kWh respectively, while in Bogota and Zonguldak, PCM 23 showed the best performance achieving energy savings of 20 741 kWh and 12 497 kWh accordingly. In Paris, Mar del Plata, and Port Elizabeth, PCM24 was found to be optimum demonstrating energy savings of 14 543 kWh, 17 868 kWh and 10 380 kWh, respectively. Finally, in Melbourne, PCM 25 resulted in the highest energy savings of 15 541 kWh accordingly. The effectiveness of PCM 22–PCM 25 can be explained by favorable outside climate conditions in this climate region. Saffari et al. (2017b) tried to find optimum PCM melting temperatures for increasing the energy-saving potential of the lightweight building located in different climates of the world. As representatives of the Cfb climate zone, the authors considered Berlin, Paris, and Johannesburg. The results showed, that in Berlin, Paris, and Johannesburg optimum PCM melting temperatures were 24.38 °C , 24.06 °C , and 25.56 °C respectively. This data is similar to the optimum PCM melting temperature range obtained in the present study. Alam et al. (2017) investigated the impact of PCM melting temperature on the thermal performance of the residential building located in the climate of Melbourne (Australia) representing the Cfb climate zone using Energy Plus software. The results of the study revealed that PCM with a melting temperature of 25 °C was the best and resulted in higher values of peak temperature drop.

For a more detailed analysis of the impact of PCM melting temperature on the energy-saving potential of the building, monthly energy consumption of the most effective PCM and least effective PCM were considered. For demonstration purposes, the cities of Bilbao and Zonguldak were selected. In Bilbao and Zonguldak the most effective performance was demonstrated by PCM 22 and PCM 23 respectively, while PCM 30 resulted in the lowest energy-saving performance for both cities. Fig. 15 summarizes the monthly energy consumption of the most and least effective PCMs for Bilbao and Zonguldak. According to the data obtained, it can be noticed that in Bilbao in June, July, August, and September both PCM 22 and PCM 30 demonstrated similar performance, while in the remaining months, PCM 22 resulted in slightly lower energy consumption values. In Zonguldak, most of the time except for March, April, and May both PCMs (PCM 23 and PCM 30) showed similar performance. In March, April, and May, PCM 23 resulted in slightly lower energy consumption values. To analyze the performance of the most effective and least effective PCMs,

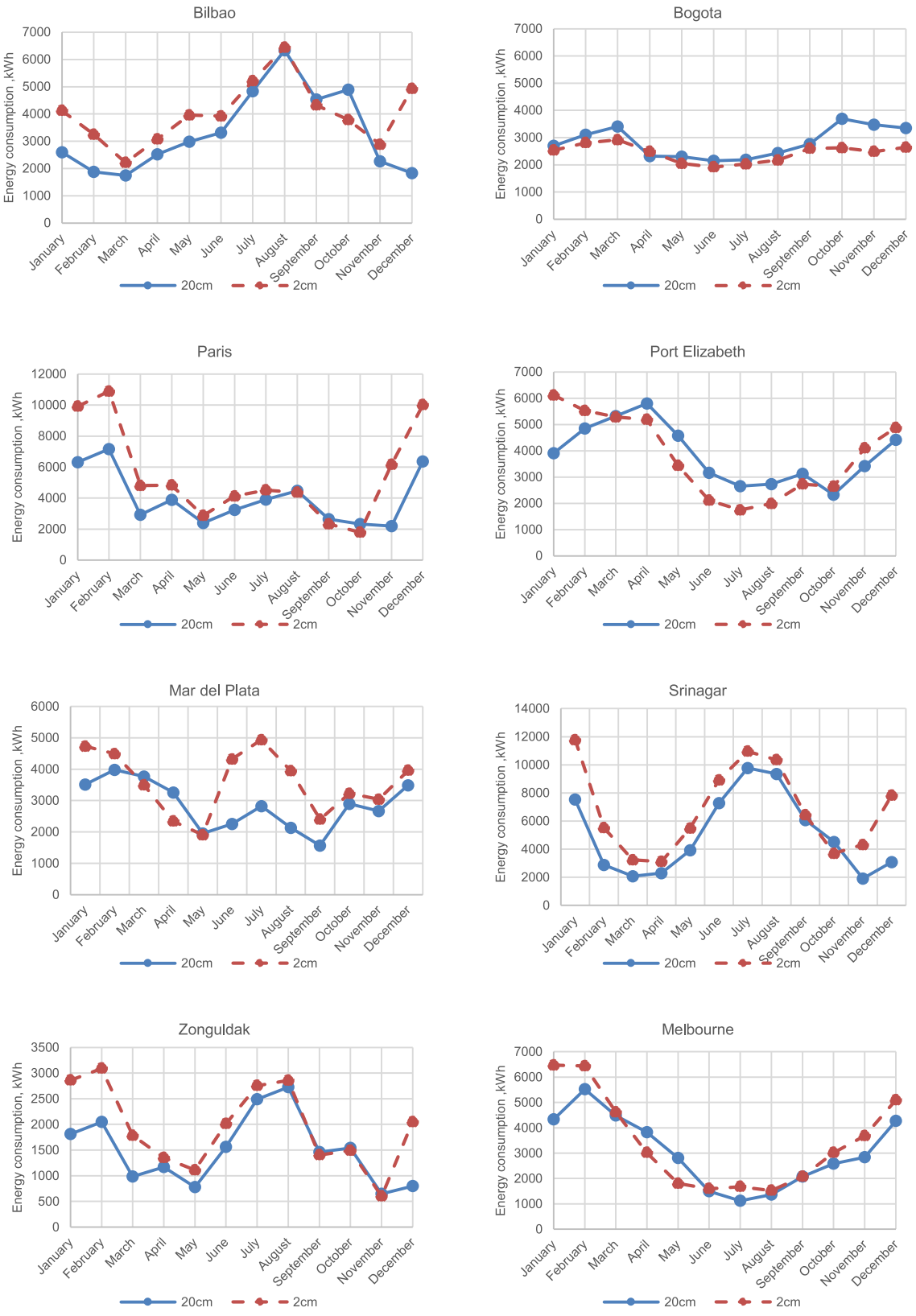

Fig. 11. Energy consumption for 2 cm and 20 cm cases.

the inner surface analysis was conducted. For each city, two months were considered: one month when both the most and least effective PCMs demonstrated the same performance, and one month when the most effective PCM showed slightly better performance. Fig. 16 summarizes the results of the inner surface analysis for Bilbao and Zonguldak for months when the most and least effective PCMs demonstrate similar performance in terms of energy consumption, which are August and July respectively. The

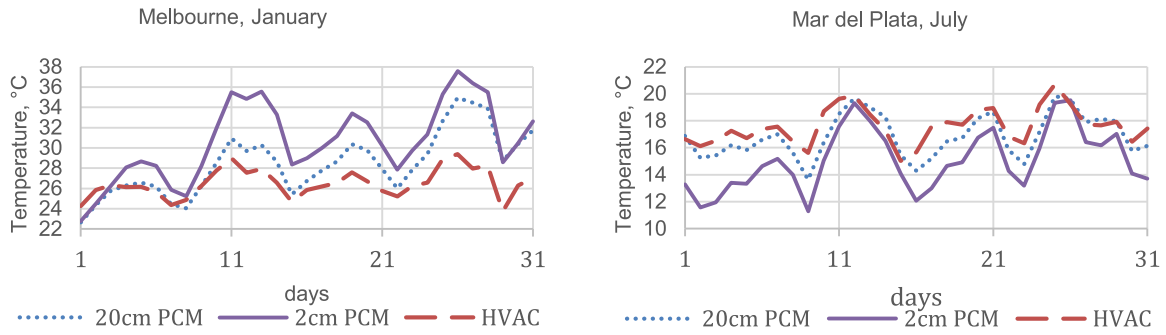

Fig. 12. Daily inner surface analysis: effectiveness of 20 cm PCM (Melbourne and Mar del Plata).

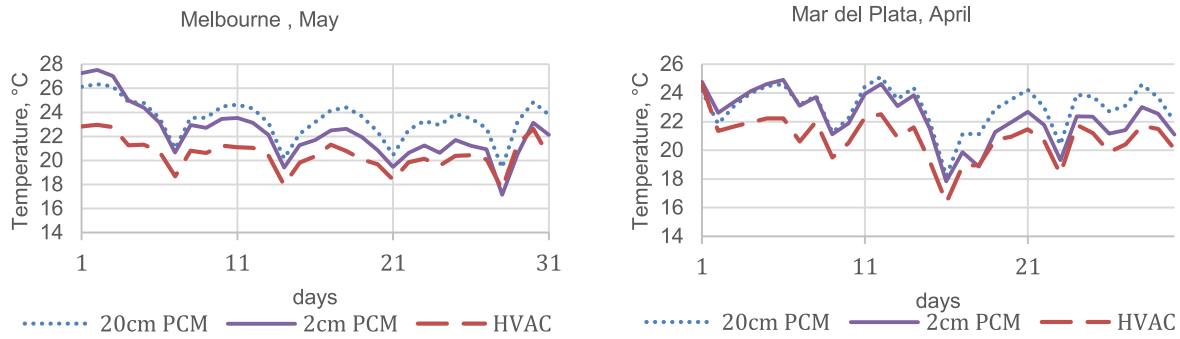

Fig. 13. Daily inner surface analysis: effectiveness of 2 cm PCM (Melbourne and Mar del Plata).

results show that in the selected cities both PCMs work against HVAC, demonstrating a huge gap in inner surface temperature between PCM cases and HVAC cases. This explains similar energy consumption values for both (least and most effective) PCMs. Fig. 17 represents the results of the inner surface analysis for Bilbao and Zonguldak for months when the most effective PCM demonstrated slightly better performance, which are November and April, respectively. According to the results presented, it can be noticed that in Bilbao, most of the time the gap between the HVAC case and PCM 22 is notably smaller compared to the PCM 30 case. This demonstrates the effectiveness of PCM 22 in supporting favorable thermal comfort conditions inside the building similar to the HVAC system. In Zonguldak during some days of the month, the gap between the temperature for the HVAC case and PCM 23 case was smaller compared to the HVAC case, demonstrating the more effective performance of the PCM 23 over PCM 30.

3.4. Impact of optimum PCMs on the thermal comfort

In this section, the impact of the optimum PCMs on the PMV values was evaluated. For demonstration purposes, four days of the summer period (June 12–June 15) were selected. Despite thermal comfort was set to PMV values ranging from −0.5 to +0.5, the integration of the PCM slightly affected PMV values. Fig. 18 summarizes the results of the PMV values for no PCM and optimum PCM cases during four consecutive days for selected cities. From the data presented, it can be noticed that for all cities, the PMV pattern for no PCM and optimum PCM cases is similar. However, during the periods ranging from 00:00 h to 06:00 h of each day, PMV values for optimum PCM cases are more towards zero compared to no PCM case. It means that PCM is working and helps to improve the thermal conditions inside the building by moving the neutral sensation category. Overall, despite the HVAC setpoints, the integration of PCM slightly helps to achieve the level of thermal comfort inside the office building considered for analysis.

3.5. The sensitivity analysis on PCM melting temperature selection

Based on the results of the previous section it was concluded that PCMs with a melting temperature in the range from 22 °C to 25 °C are optimum for eight cities representing the Cfb climate zone. However, the obtained PCM melting temperature range is still wide, and random selection of the PCM melting temperature from this range may notably affect the energy performance of the building. Therefore, this section investigates to what extent the random selection of the PCM melting temperature from the obtained optimum range can affect the energy performance of the building. For this purpose, for each city, PCMs resulting in the lowest and the highest annual energy savings within the optimum range (22–25 °C) were selected and analyzed. The list of the most effective and least effective PCMs out of the proposed optimum PCM range is provided in Table 5, whereas the energy savings and ECR values for those PCMs are summarized in Fig. 19. From the results presented it can be seen that differences in ECR between the most effective and least effective PCMs are 3.6%, 1.5%, 2.4%, 1.2%, 1.1%, 0.9%, 0.6% and 0.4% in Bogota, Port Elizabeth, Mar del Plata, Melbourne, Paris, Bilbao, Srinagar, and Zonguldak respectively. Bogota demonstrated the highest ECR difference, which means that it is sensitive to the selection of PCM melting temperature and it is crucial to select the optimum PCM out of the provided range. In contrast, Zonguldak is characterized by the lowest drop in ECR values of the top-1 and top-4 PCMs, which in turn means that it is not sensitive, and all the PCMs from the PCM 22-PCM 25 range are equally effective. The contrast in the results for Zonguldak and Bogota can be explained by a difference in outside climate conditions. Fig. 20 demonstrates monthly outside air temperature values for Bogota and Zonguldak, while Fig. 21 represents the monthly direct normal solar radiation for these cities.

In order to quantify the impact of the steadiness of climate conditions on the sensitivity of energy savings to the selection of PCM melting temperature out of the suggested optimum PCM melting temperature range, a standard deviation of outside air

Fig. 14. ES and ECR for PCM 18-PCM 30 cases.

temperature and direct solar radiation as well as average savings drop (ASD) were calculated. The steadiness of climate conditions is represented by the standard deviation of the outside air temperature and direct solar radiation, while the quantitative evaluation of the sensitivity of energy savings to the selection of optimum PCM melting temperature is represented by ASD. The higher ASD value shows higher sensitivity values. Figs. 22 and 23 represent the relationship between ASD and outside air temperature and solar radiation standard deviation respectively for all cities. Overall, it is seen that in cities, characterized by high standard deviation values for outside air temperature and solar radiation, ASD values were notably low, while in cities with low standard deviation values for outside climate conditions ASD values were comparatively high. The results demonstrate that the energy performance of the building in Bogota is quite sensitive to the selection of PCM melting temperature and it is

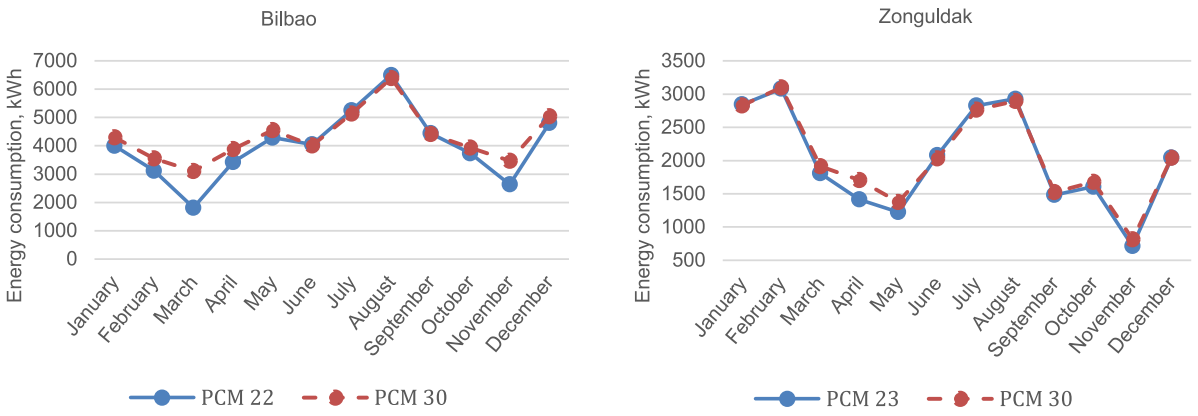

Fig. 15. Monthly energy consumption of most and least effective PCMs (Bilbao and Zonguldak).

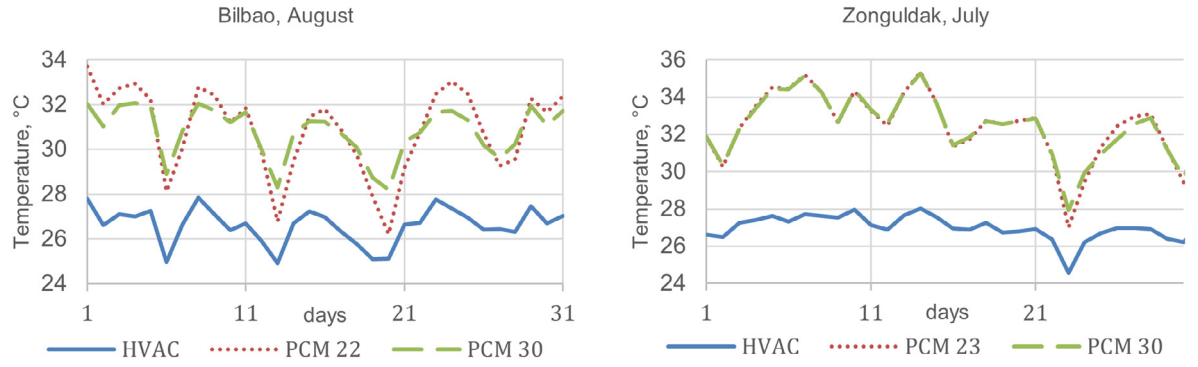

Fig. 16. Daily inner surface analysis: ineffectiveness of optimum PCM (Bilbao and Zonguldak).

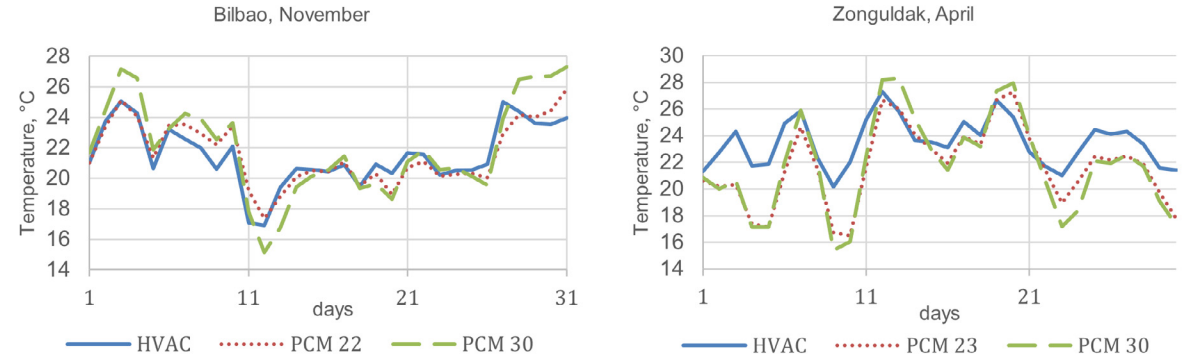

Fig. 17. Daily inner surface analysis: effectiveness of optimum PCM (Bilbao and Zonguldak).

related to the steadiness of the climate conditions. Thus, it can be concluded that the sensitivity of the energy performance depends on the steadiness of outside climate conditions. Therefore, this factor should be considered in the PCM melting temperature optimization process.

3.6. Energy performance of the building integrated with real PCMs

In this section, the impact of real PCMs on the annual energy consumption of office building located in different cities of Cfb climate zones was investigated. Fig. 24 summarizes the results of the energy simulations for all cities. Overall, in all cities, PCM 25-r resulted in the highest energy savings, reaching the values of 14 013 kWh, 21 404 kWh, 16 024 kWh, 11 263 kWh, 20 081 kWh, 22 535 kWh, 14 225 kWh, and 17 303 kWh in Bilbao, Bogota, Paris, Port Elizabeth, Mar del Plata, Srinagar, Zonguldak, and Melbourne respectively. In all cities except for Bogota and Port Elizabeth, PCM 22-r resulted in the lowest annual energy savings, while in the remaining cities PCM 21-r demonstrated the worst performance. However, it is worth mentioning that in all cities the difference in energy savings for PCM 21-r and PCM 22-r cases

Table 5
List of most effective and least effective PCMs for all cities from the selected optimum melting temperature range.

	Most effective PCM	Least effective PCM
Bogota	PCM 23	PCM 22
Port Elizabeth	PCM 24	PCM 22
Mar del Plata	PCM 24	PCM 22
Melbourne	PCM 25	PCM 22
Paris	PCM 24	PCM 22
Bilbao	PCM 22	PCM 25
Srinagar	PCM 22	PCM 25
Zonguldak	PCM 23	PCM 25

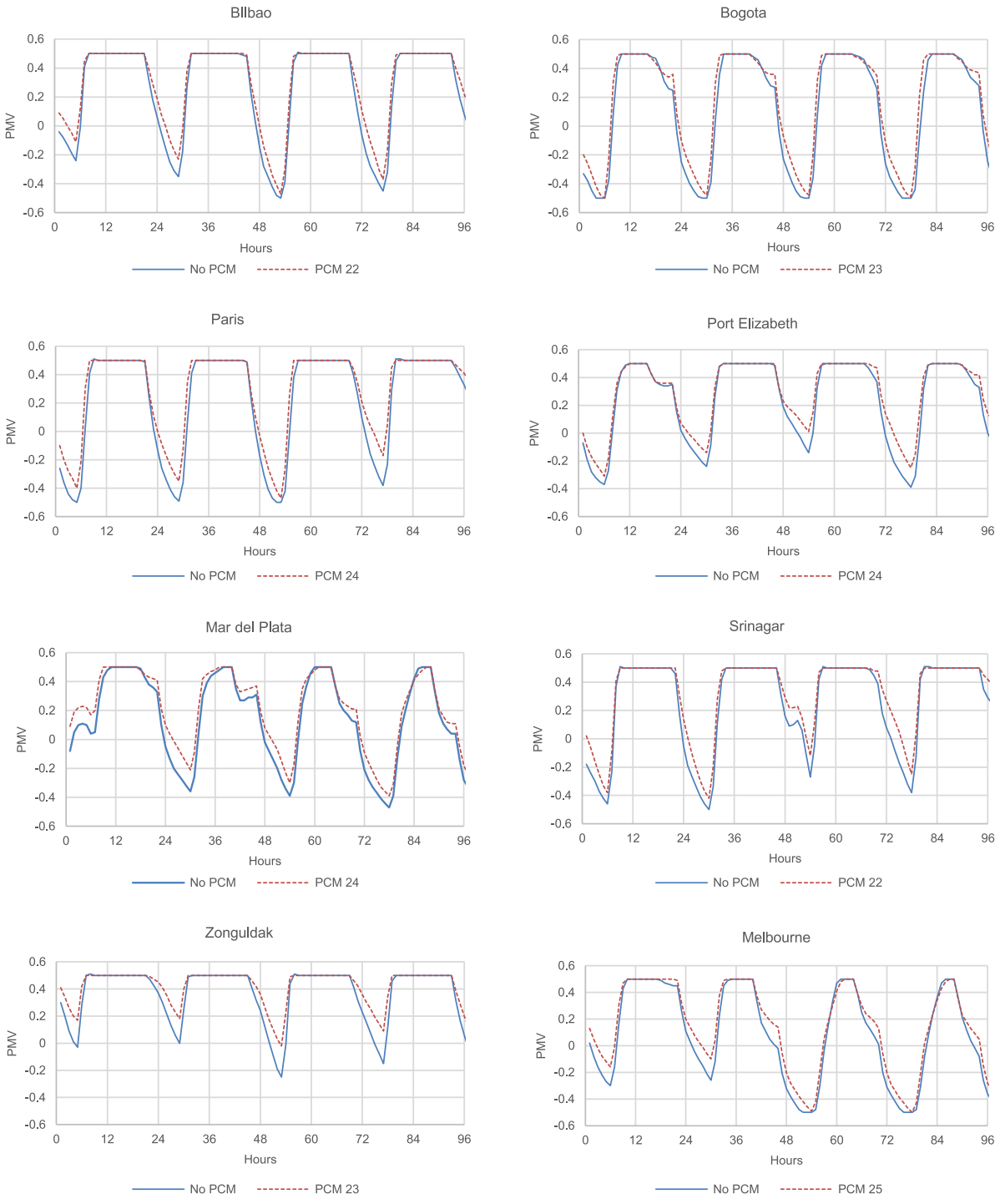

Fig. 18. PMV for No PCM and optimum PCMs for four consecutive days (June 12–June 15).

is very small. According to the data presented, it can be noticed that Port Elizabeth is characterized by the lowest annual energy savings for all PCMs, and Srinagar is characterized by the highest energy savings for all PCMs.

For more detailed analysis, the monthly energy savings of the most effective and least effective PCMs were considered for Srinagar and Port Elizabeth (Fig. 25). According to the data presented, in Port Elizabeth, PCM 25-r resulted in comparatively higher energy savings in all months except for April. It reached the maximum energy savings of up to 1766 kWh in October. In Srinagar, in the period from March to July, and from August to October, PCM 25-r demonstrated comparatively higher energy savings, while in the remaining months both PCM 22-r and PCM 25-r showed similar performance. The maximum energy savings produced by the integration of PCM 25-r were observed in November, it reached the value of 3489 kWh. To analyze the performance of the most effective and least effective PCMs, the inner surface analysis was conducted. For each city, two months were considered: one month when both the most and least effective PCMs demonstrated the same performance, and one month when the most effective PCM showed slightly better performance. Fig. 26 represents the results of the inner surface analysis for Port Elizabeth and Srinagar for months when

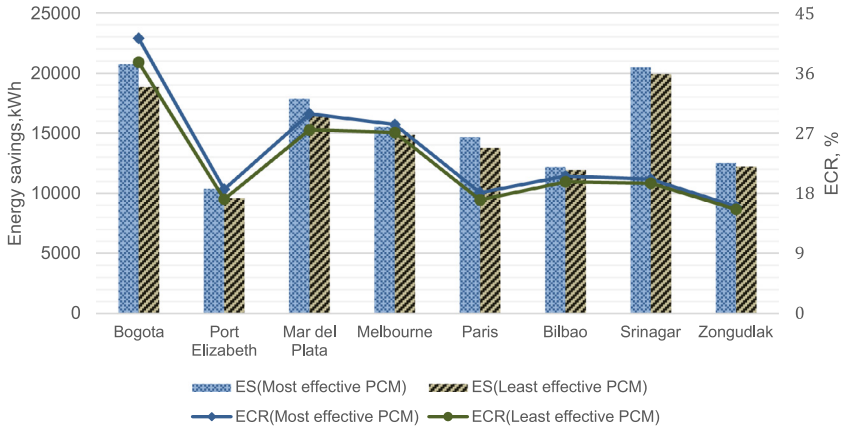

Fig. 19. ES and ECR for least and most effective PCMs.

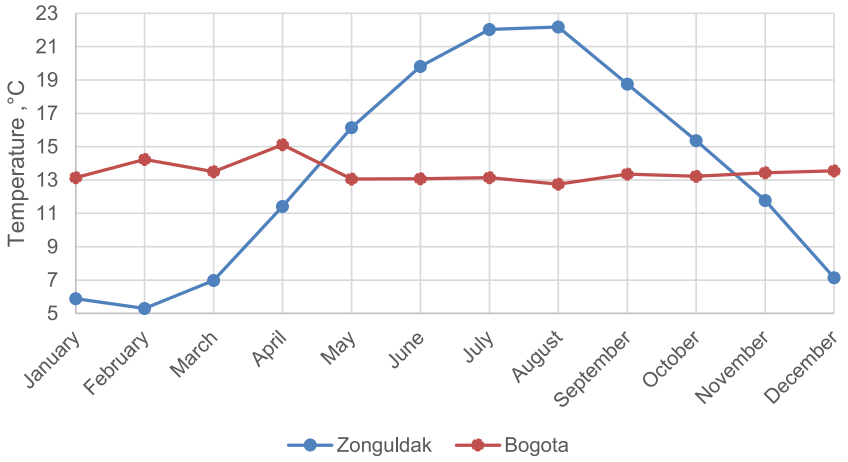

Fig. 20. Monthly outside air temperature.

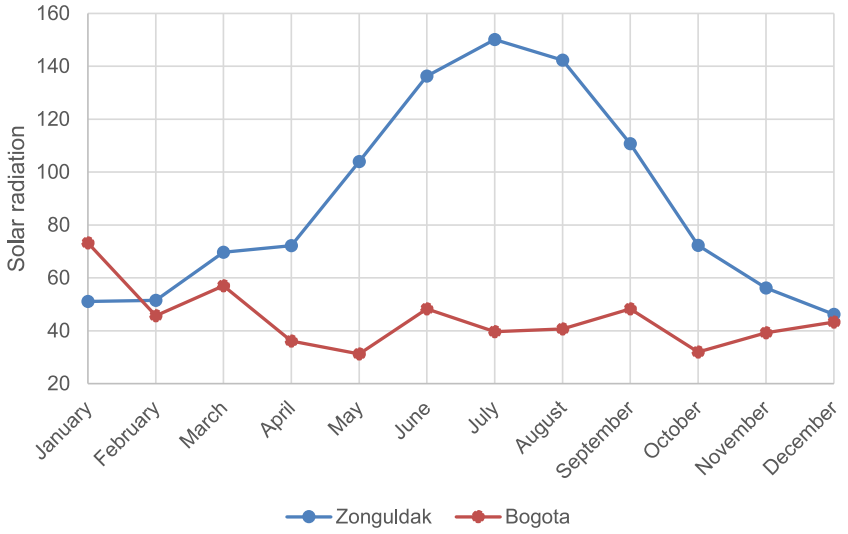

Fig. 21. Monthly direct normal solar radiation.

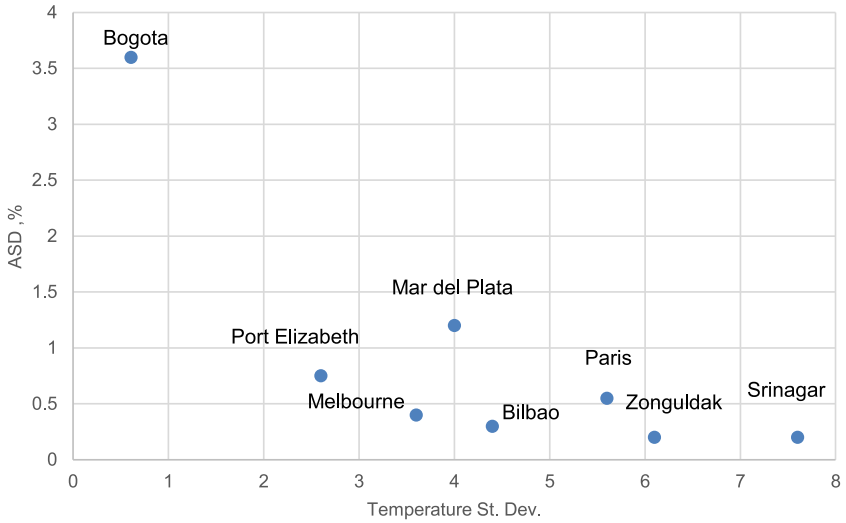

Fig. 22. ASD vs Temperature St. Dev.

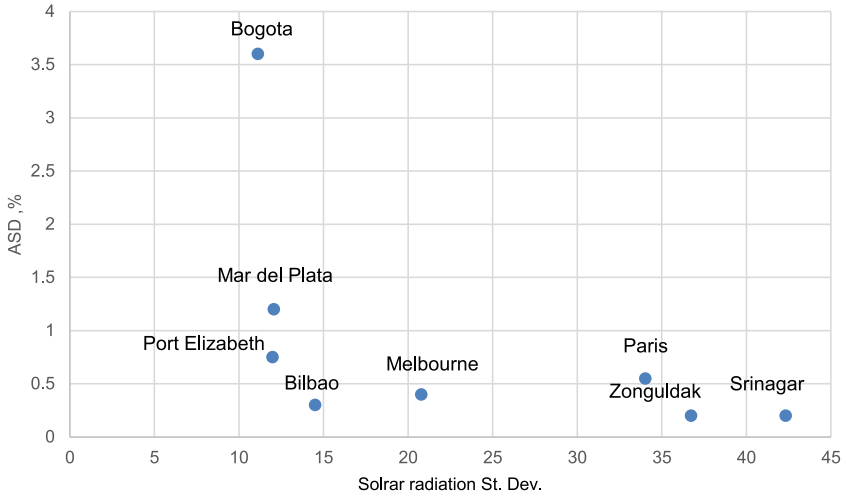

Fig. 23. ASD vs Solar radiation St. Dev.

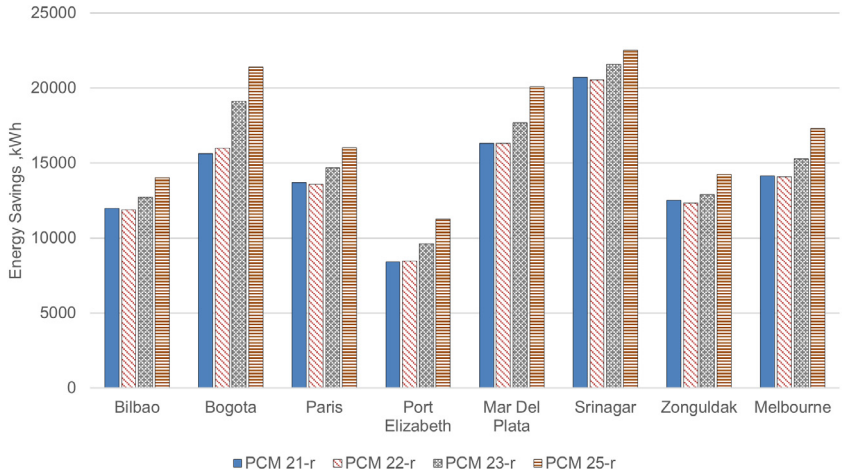

Fig. 24. Annual energy savings for real PCMs.

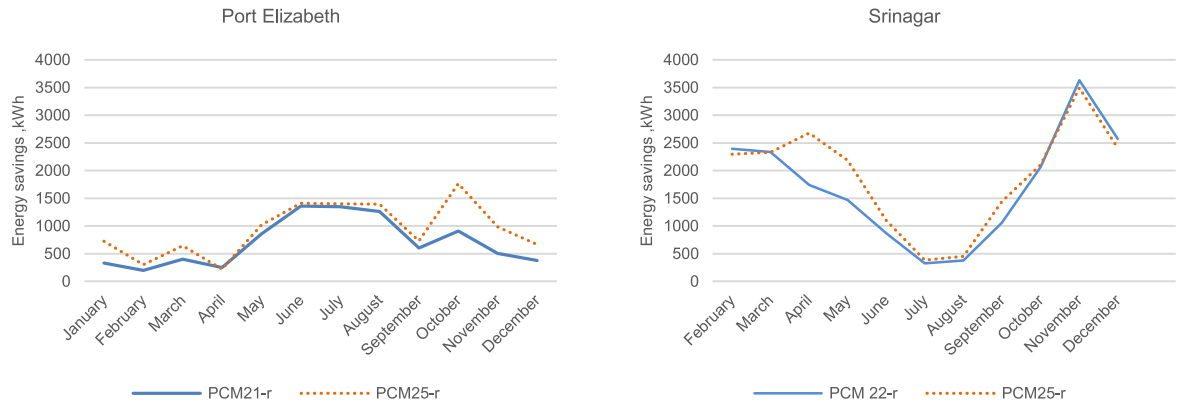

Fig. 25. Monthly energy savings for Port Elizabeth and Srinagar.

the most effective real PCMs demonstrated slightly better performance, which are October and April, respectively. The results show that in Srinagar, most of the time the gap between the HVAC case and PCM 25-r is notably smaller compared to the PCM 22-r case. This demonstrates the effectiveness of PCM 25-r in supporting favorable thermal comfort conditions inside the building similar to the HVAC system. In Port Elizabeth during some days of the month, the gap between the temperature for the HVAC case and PCM 25-r case was slightly smaller compared to the HVAC case, demonstrating the more effective performance of the PCM 25-r over PCM 21-r. Fig. 27 represents the results of the inner surface analysis for Port Elizabeth and Srinagar for months when the most and least effective PCMs demonstrate similar performance in terms of energy savings, which are April and October respectively. According to the data presented in the selected cities both the most and least effective PCMs work against HVAC, demonstrating a huge gap in inner surface temperature between PCM cases and HVAC case, which explains the same amount of energy savings produced by the most effective and least effective PCMs.

Comparing the energy performance of real PCMs with the energy performance of fictitious PCMs, several changes can be observed. For fictitious PCMs, the optimum melting temperature varied from city to city in the range from 22 °C to 25 °C , while for real PCMs, PCM with the melting temperature of 25 °C showed the best performance in terms of energy savings in all cities selected for analysis. The possible reason behind this is the fact that fictitious PCMs had the same heat storage capacity, while real PCMs considered in the present study possess various heat storage capacities, and PCM 25-r has the highest value of 210 kJ/kg compared to the values of heat storage capacity for PCM 21-r, PCM 22-r, and PCM 24-r which are 190 kJ/kg, 190 kJ/kg, and 160 kJ/kg respectively. It is therefore recommended to investigate the sensitivity of energy performance to the selection of thermophysical properties of PCM.

3.7. Economic and environmental analysis of the PCM integration

In this section, the economic feasibility of PCM integrated buildings in eight cities in the Cfb climate zone was evaluated using a static payback period indicator. The economic analysis was conducted for the optimized thickness of 2 cm and optimum real PCM so that the volume of the used PCM was 39.643 m^3. Table 5 summarizes the energy savings, cost of electricity in USD per kWh and equivalent CO_2 emissions in kg per kWh for each city selected for analysis. Fig. 28 represents the payback period for each city. According to the data presented, for all cities except for Zonguldak and Mar del Plata, the payback period varied from 9 to 19 years. In Zonguldak and Mar del Plata, the payback period was 77.8 and 43.8 years respectively. These values can be explained by the comparatively low price for electricity in these cities equal to 0.031 USD/kWh and 0.039 USD/kWh for Zonguldak and Mar del Plata respectively. Although the cost of electricity in Mar del Plata is similar to that of Zonguldak, the payback period is considerably smaller because the integration of PCM in this city resulted in notably higher energy savings. The lowest payback period of 9.5 years was observed in Bilbao. The reason behind this is the comparatively high cost of electricity in this city, which makes the integration of PCM an energy-efficient and cost-effective solution. In Bogota and Paris, the payback period was around 11 years, it is also related to a comparatively higher price for electricity and higher energy savings in these cities.

For environmental analysis, the amount of CO_2 emissions that can be reduced due to the integration of PCM was determined. For this, the quantities of CO_2 emissions caused by electricity generation in various countries were used. Fig. 29 summarizes the results of the CO_2 equivalent savings for selected cities. The results show that Srinagar and Melbourne are characterized by the largest amount of CO_2 savings caused by the integration of PCM, reaching the values of 20 507 kg/year and 13 808 kg/year respectively. This trend can be explained by the largest amount of CO_2 emissions caused by the production of 1 kWh of electricity in Srinagar (India) and Melbourne (Australia) shown in Table 6. The main source of energy in both India and Australia is coal. As far as Paris (France) is concerned, it is characterized by the lowest amount of CO_2 savings, reaching the value of 1025 kg/year. From Table 6 it is seen that Paris has the lowest amount of CO_2 emissions caused by the generation of electricity. The possible reason behind this is that 71% of total power generated in France is obtained from nuclear power plants (Anon, 2022), which do not produce greenhouse gas emissions. Overall, the results demonstrate that the utilization of PCM in most of the cities in the Cfb climate zone is economically and environmentally feasible.

4. Conclusions and recommendations

In the present study optimization of PCM layer thickness as well as PCM melting temperature for increasing the annual energy savings of the office building located in eight cities of Cfb climate zone was accomplished using Design Builder software under Fanger model thermal comfort conditions. The sensitivity of the energy-saving potential of the building to the selection of PCM melting temperature was analyzed and quantified by using a novel indicator of average savings drop (ASD). Then, the impact of real PCMs on the energy performance of the PCM integrated buildings was studied. Additionally, the economic and environmental analysis of the PCM integrated buildings was provided. The main findings are summarized below:

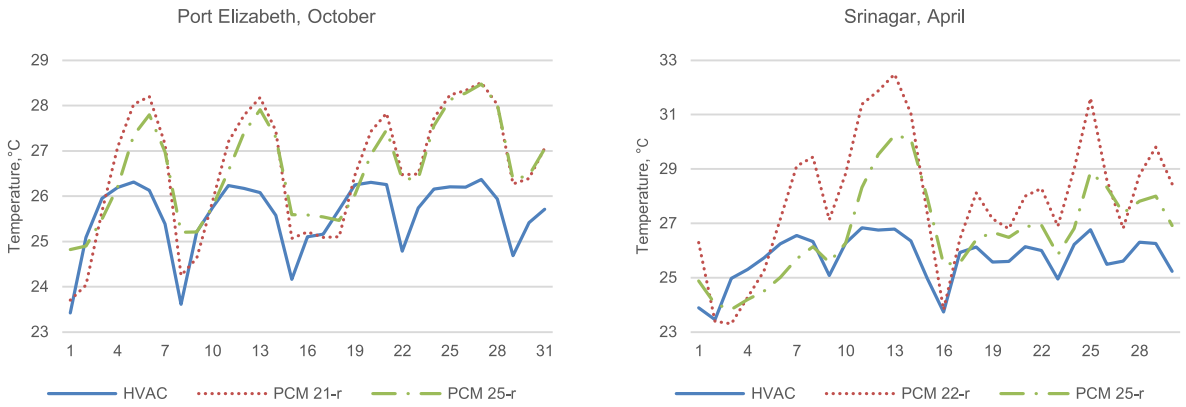

Fig. 26. Daily inner surface analysis: effectiveness of optimum PCM (Port Elizabeth and Srinagar).

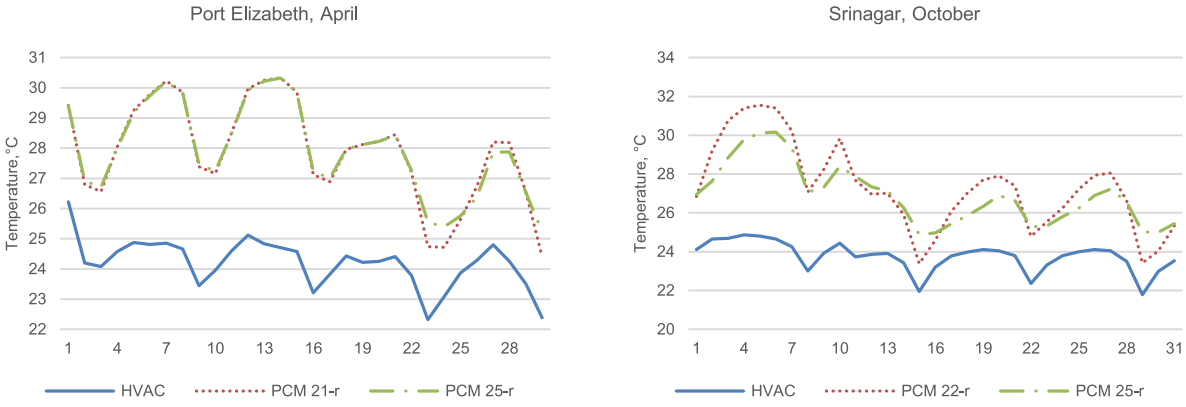

Fig. 27. Daily inner surface analysis: ineffectiveness of optimum PCM (Port Elizabeth and Srinagar).

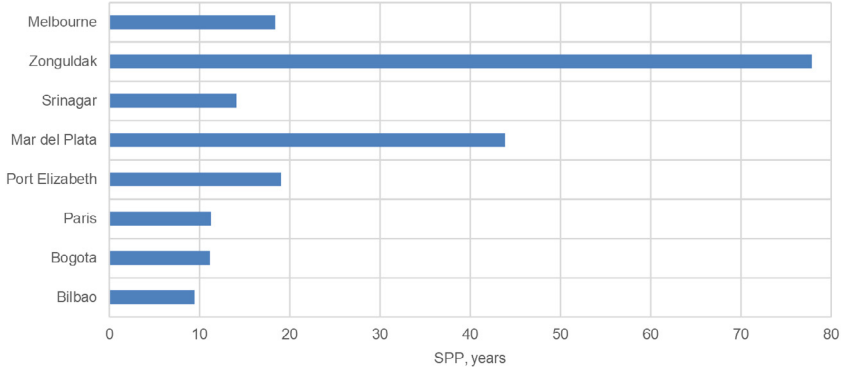

Fig. 28. SPP for selected cities.

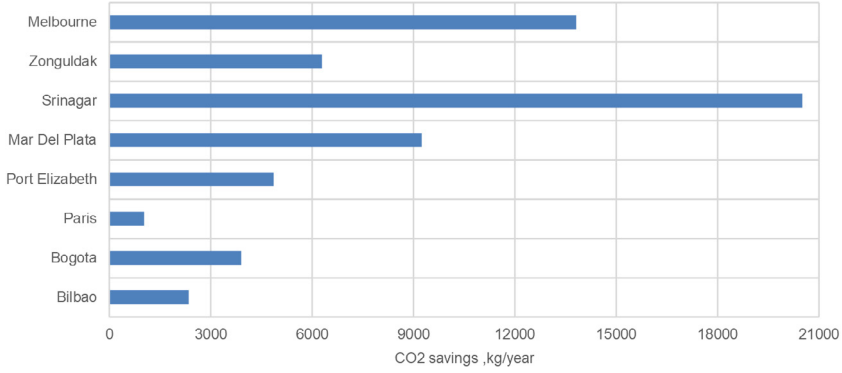

Fig. 29. Amount of annual CO_2 savings produced by the integration of PCM.

Table 6
Summary of energy savings, electricity cost per kWh and amount of CO_2 emissions per kWh for selected cities.

City	Country	ES, kWh	Cost of electricity, USD/kWh	CO_2 emissions, kg/kWh
Bilbao	Spain	14013.98	0.26[a]	0.167
Bogota	Columbia	21404.98	0.144[b]	0.182
Paris	France	16024.92	0.19[c]	0.064
Port Elizabeth	South Africa	11263.22	0.16[d]	0.432
Mar Del Plata	Argentina	20081.73	0.039[e]	0.46
Srinagar	India	22535.85	0.108[f]	0.91
Zonguldak	Turkey	14225.34	0.031[g]	0.442
Melbourne	Australia	17303.38	0.108[h]	0.798

[a] https://www.costtotravel.com/cost/electricity-in-bilbao.
[b] https://www.globalpetrolprices.com/Colombia/electricity_prices/.
[c] https://en.selectra.info/energy-france/guides/electricity/tariffs.
[d] https://mybroadband.co.za/news/energy/387796-the-south-african-cities-with-the-most-expensive-electricity.html.
[e] https://www.globalpetrolprices.com/Argentina/electricity_prices/.
[f] https://www.globalpetrolprices.com/India/electricity_prices/.
[g] https://www.costtotravel.com/cost/electricity-in-zonguldak.
[h] https://www.globalpetrolprices.com/Australia/electricity_prices/.

- In all cities representing the Cfb climate zone PCM layer with the thickness of 20 cm produced the highest energy savings, whereas the PCM layer with the thickness of 2 cm resulted in the highest energy savings growth per unit thickness. It was selected as optimum because it was more efficient and cost-effective.
- The results of the PCM melting temperature optimization revealed that for considered Cfb climate zone cities, fictitious PCMs with the melting temperature ranging from 22 °C to 25 °C demonstrated more effective performance. The effectiveness of fictitious PCMs with this melting temperature range can be explained by the fact that most of the time outdoor climate conditions were favorable for these PCMs, resulting in the highest cumulative annual energy savings. The surface analysis supported the above-mentioned statement showing that in the months with the comparatively higher energy savings, the application of optimum PCM resulted in the thermal performance similar to the HVAC case.
- The integration of novel indicators of ASD allowed quantification of the sensitivity of the energy savings to the selection of PCM melting temperature, while the standard deviation of outside air temperature and direct solar radiation quantified the steady-state climate conditions of each city. The relationship between ASD and steadiness of climate conditions showed that in cities, characterized by high standard deviation values for outside air temperature and solar radiation, ASD values were notably low, while in cities with low standard deviation values for outside climate conditions, ASD values were comparatively high.
- Cities characterized by steady-state climate conditions are more sensitive to the selection of PCM melting temperature out of the specified PCM melting temperature range. For example, Bogota had notably stable climate conditions compared to other cities, which explains its high sensitivity to the selection of the optimum PCM melting temperature.
- The analysis of the impact of real PCMs on the energy performance of the buildings showed that PCM 25-r resulted in the highest energy savings in all cities. The economic analysis showed that for most cities, the integration of PCM into the building envelope is an economically feasible option. In Bilbao, Bogota, Paris, Port Elizabeth, Srinagar, and Melbourne, the payback period was in the range of 9 to 19 years, whereas in Zonguldak and Mar del Plata it was 77.8 and 43.8 years respectively. Finally, from the environmental analysis, it was revealed that the integration of PCM to the buildings located in the Cfb climate zone is environmentally feasible and may contribute to reducing the building-related CO_2 emissions.
- For future studies, the concept of introduced sensitivity analysis of energy performance to the selection of PCM melting temperature can be extended and verified by applying it to other climate regions and different building types. The role of sensitivity analysis of energy performance to the selection of thermo-physical properties of PCM should be investigated. Also, the impact of climate change on sensitivity analysis of energy performance to the selection of PCM melting temperature can be evaluated. Finally, further investigation regarding the optimization of PCM melting temperature for cities with steady outside temperature and solar radiation is recommended.

CRediT authorship contribution statement

Abylaikhan Bozzhigitov: Writing – original draft, Investigation, Methodology, Software, Visualization. **Shazim Ali Memon:** Conceptualization, Methodology, Writing – review & editing, Project administration, Funding acquisition. **Indira Adilkhanova:** Writing – review & editing, Visualization.

Declaration of competing interest

The authors declare that they have no known competing financial interests or personal relationships that could have appeared to influence the work reported in this paper.

Acknowledgments

This research was supported by Nazarbayev University, Kazakhstan Faculty development competitive research grants numbers 021220FD0651.

References

Ahangari, M., Maerefat, M., 2019. An innovative PCM system for thermal comfort improvement and energy demand reduction in building under different climate conditions. Sustain. Cities Soc. 44, 120–129. http://dx.doi.org/10.1016/J.SCS.2018.09.008.

AHSRAE-55-2010, 2010. ASHRAE STANDARD. Thermal Environment Conditions for Human Occupancy. 2010.

Alam, M., Jamil, H., Sanjayan, J., Wilson, J., 2014. Energy saving potential of phase change materials in major Australian cities. 78, pp. 192–201.

Alam, M., Sanjayan, J., Zou, PXW., Ramakrishnan, S., Wilson, J., 2017. Evaluating the passive and free cooling application methods of phase change materials in residential buildings: A comparative study. Energy Build. 148, 238–256. http://dx.doi.org/10.1016/j.enbuild.2017.05.018.

Anon, 2006. Introduction to computational fluid dynamics. Choice Rev. Online 43, http://dx.doi.org/10.5860/choice.43-4683.

Anon, 2022. Production of electricity in France in 2019–2020, by energy source. Statista https://www.statista.com/statistics/768066/electricity-production-france-source/ (accessed April 1, 2022).

Arıcı, M., Bilgin, F., Nižetić, S., Karabay, H., 2020. PCM integrated to external building walls: AN optimization study on maximum activation of latent heat. Appl. Therm. Eng. 165, 114560. http://dx.doi.org/10.1016/j.applthermaleng.2019.114560.

Ascione, F., Bianco, N., De Masi, R.F., de Rossi, F., Vanoli, G.P., 2014. Energy refurbishment of existing buildings through the use of phase change materials: Energy savings and indoor comfort in the cooling season. Appl. Energy 113, 990–1007. http://dx.doi.org/10.1016/J.APENERGY.2013.08.045.

Bimaganbetova, M., Memon, SA., Sheriyev, A., 2019. Performance evaluation of phase change materials suitable for cities representing the whole tropical savanna climate region. Renew. Energy http://dx.doi.org/10.1016/J.RENENE.2019.10.046.

Cui, H., Memon, SA., Liu, R., 2015. Development, mechanical properties and numerical simulation of macro encapsulated thermal energy storage concrete. Energy Build. 96, 162–174. http://dx.doi.org/10.1016/j.enbuild.2015.03.014.

Design Builder, 2020. Welcome to DesignBuilder V6. https://designbuilder.co.uk/helpv6.0/#GetStarted.htm?TocPath=Get%2520Started%257C_____0 (accessed November 20, 2020).

Designing Buildings, 2020. Operative temperature. https://www.designingbuildings.co.uk/wiki/Operative_temperature. (accessed February 3, 2020).

Djongyang, N., Tchinda, R., Njomo, D., 2010. Thermal comfort: A review paper. Renew. Sustain. Energy Rev. 14, http://dx.doi.org/10.1016/j.rser.2010.07.040.

Energy Plus, 2022. EnergyPlus Thermal comfort. https://designbuilder.co.uk/helpv2/Content/Thermal_Comfort.htm (accessed January 15, 2022).

Hyoung Kyu, C., 2015. Introduction to Numerical Analysis.

IEA, 2019. Energy efficiency: Buildings. https://www.iea.org/topics/energyefficiency/buildings/. (accessed August 15, 2019).

Jangeldinov, B., Memon, SA., Kim, J., Kabdrakhmanova, M., 2020. Evaluating the energy efficiency of PCM-integrated lightweight steel-framed building in eight different cities of warm summer humid continental climate. Adv. Mater. Sci. Eng. 2020.

Kenzhekhanov, S., Memon, SA., Adilkhanova, I., 2020. Quantitative evaluation of thermal performance and energy saving potential of the building integrated with PCM in a subarctic climate. Energy 192, 116607. http://dx.doi.org/10.1016/J.ENERGY.2019.116607.

Kishore, RA., Bianchi, MVA., Booten, C., Vidal, J., Jackson, R., 2020. Optimizing PCM-integrated walls for potential energy savings in U.S.. Build. Energy Build. 226, 110355. http://dx.doi.org/10.1016/j.enbuild.2020.110355.

Lei, J., Yang, J., Yang, E.H., 2016. Energy performance of building envelopes integrated with phase change materials for cooling load reduction in tropical Singapore. Appl. Energy 162, 207–217. http://dx.doi.org/10.1016/j.apenergy.2015.10.031.

Markarian, E., Fazelpour, F., 2019a. Multi-objective optimization of energy performance of a building considering different configurations and types of PCM. Sol Energy 191, 481–496. http://dx.doi.org/10.1016/j.solener.2019.09.003.

Markarian, E., Fazelpour, F., 2019b. Multi-objective optimization of energy performance of a building considering different configurations and types of PCM. Sol. Energy 191, 481–496. http://dx.doi.org/10.1016/j.solener.2019.09.003.

Mathew, A., Sreekumar, S., Khandelwal, S., Kumar, R., 2019. Prediction of land surface temperatures for surface urban heat island assessment over Chandigarh city using support vector regression model. Sol. Energy 186, 404–415. http://dx.doi.org/10.1016/j.solener.2019.04.001.

Mi, X., Liu, R., Cui, H., Memon, SA., Xing, F., Lo, Y., 2016. Energy and economic analysis of building integrated with PCM in different cities of China. Appl. Energy 175, 324–336. http://dx.doi.org/10.1016/j.apenergy.2016.05.032.

Mohseni, E., Tang, W., 2021. Parametric analysis and optimisation of energy efficiency of a lightweight building integrated with different configurations and types of PCM. Renew. Energy 168, 865–877. http://dx.doi.org/10.1016/j.renene.2020.12.112.

OECD, 2019. Compare your country - climate change mitigation policies. http://www.compareyourcountry.org/climate-policies?cr=oecd&lg=en&page=2 (accessed August 12, 2019).

Peng, B., Huang, G., Wang, P., Li, W., Chang, W., Ma, J., et al., 2019. Effects of thermal conductivity and density on phase change materials-based thermal energy storage systems. Energy 172, 580–591. http://dx.doi.org/10.1016/J.ENERGY.2019.01.147.

Ramakrishnan, S., Wang, X., Alam, M., Sanjayan, J., Wilson, J., 2016. Parametric analysis for performance enhancement of phase change materials in naturally ventilated buildings. Energy Build 124, 35–45. http://dx.doi.org/10.1016/j.enbuild.2016.04.065.

Rubitherm, 2020. Phase change materials. https://www.rubitherm.eu/en//index.html (accessed October 29, 2020).

Saffari, M., De Gracia, A., Ushak, S., Cabeza, L.F., 2016. Economic impact of integrating PCM as passive system in buildings using Fanger comfort model. Energy Build. 112, 159–172. http://dx.doi.org/10.1016/j.enbuild.2015.12.006.

Saffari, M., de Gracia, A., Fernández, C., Cabeza, LF., 2017a. Simulation-based optimization of PCM melting temperature to improve the energy performance in buildings. Appl. Energy 202, 420–434. http://dx.doi.org/10.1016/j.apenergy.2017.05.107.

Saffari, M., de Gracia, A., Fernández, C., Cabeza, LF., 2017b. Simulation-based optimization of PCM melting temperature to improve the energy performance in buildings. Appl. Energy 202, 420–434. http://dx.doi.org/10.1016/j.apenergy.2017.05.107.

Santamouris, M., 2014. Solar thermal technologies for buildings: The state of the art. http://dx.doi.org/10.4324/9781315074467.

Souayfane, F., Fardoun, F., Biwole, PH., 2016. Phase change materials (PCM) for cooling applications in buildings: A review. Energy Build 129, 396–431. http://dx.doi.org/10.1016/j.enbuild.2016.04.006.

Tabares-Velasco, PC., Christensen, C., Bianchi, M., 2012. Verification and validation of EnergyPlus phase change material model for opaque wall assemblies. Build. Environ. 54, 186–196. http://dx.doi.org/10.1016/j.buildenv.2012.02.019.

Tunçbilek, E., Arıcı, M., Krajčík, M., Nižetić, S., Karabay, H., 2020. Thermal performance based optimization of an office wall containing PCM under intermittent cooling operation. Appl. Therm. Eng. 179, 115750. http://dx.doi.org/10.1016/j.applthermaleng.2020.115750.

Xu, X., Dong, Z., Memon, SA., Bao, X., Cui, H., 2017. Preparation and supercooling modification of salt hydrate phase change materials based on $CaCl_2 \cdot 2H_2O/CaCl_2$. Mater (Basel, Switzerland) 10. http://dx.doi.org/10.3390/ma10070691.

Zhao, Q., Lian, Z., Lai, D., 2021. Thermal comfort models and their developments: A review. Energy Built. Environ. 2, 21–33. http://dx.doi.org/10.1016/j.enbenv.2020.05.007.